Robotic Leg Illusion: System Design and Human-in-the-Loop Evaluation

Dimitri Penner, Anna M. H. Abrams, Philipp Overath, Joachim Vogt, and Philipp Beckerle, *Member, IEEE*

***Abstract*—The question how humans integrate artificial lower limb devices into their body schema has distinct potential for engineering motion assistance systems, e.g., the design of robotic prostheses. Adding robotic technology to existing psychological experiments enables a deeper investigation of multisensory interaction between proprioceptive, visual, and tactile stimuli during motion. This paper reports the design and control of a robot to investigate embodiment with regard to the lower limbs. In an evaluation study, the rubber hand illusion is transferred to the whole leg for the first time. Participants performed knee bends according to three different conditions being imitated by a robotic leg. The occurrence of a robotic leg illusion was subjectively assessed by a questionnaire and objectively measured by the proprioceptive drift. Considering both metrics, the results show a successful integration of the robotic leg into the body schema. Motion synchronization appears to be a paramount factor, whereby the study indicates that acoustical stimulation might also be relevant. The interrelation between mechatronic design and control of the human-in-the-loop experiment and the factors influencing the illusion are discussed and alternative experimental setups are suggested.**

***Index Terms*—Body schema, human-in-the-loop, human–robot interaction, multisensory integration, robotic leg illusion (RobLI).**

I. Introduction

After amputation of extremities, people are encouraged to wear prostheses when starting the rehabilitation process [1] and for the rest of their lives in order to maintain mobility. Besides physical challenges of getting used to the prosthesis, users have to psychologically and socially adapt to a new self-image [2]. A prosthesis that resembles appearance and function of the real extremity might help to counteract negative psychological consequences [3]. Robotic technology is a very promising means to improve prosthetic function [4]. Nevertheless, all users undergo two central psychological changes concerning their identity: changes in perception of the own body and integration of the prosthesis into their body schema [5].

Body perception is influenced by physical, sensory, and social factors. Physically, height, contour, and other specific attributes play a role [6]. Sensory impacts relate to remaining sensitivity of the residual limb and proprioceptive changes due to limb loss. Psychologically, emotions and attitudes toward the own body must be considered [7], [8]. In contrast to the perception of the body, one's body schema is based upon somatosensory information and represents the locations of body parts and their changes in movement. Additionally, body schema subconsciously represents body kinematics and enables integration of haptic information of particular extremities with proprioceptive information [6].

In the last decades, the rubber hand illusion (RHI) [9] has shown to be a very useful experimental paradigm to explore embodiment [10]. During this experiment, participants attribute tactile sensations experienced in their hidden hand to a rubber hand they observe being stimulated likewise. Most participants experience that the rubber hand has become part of their body given the artificial hand is in an anatomically plausible position to the real hand and within a distance of maximally 0.3 m [11]–[14]. Moreover, felt stimulation of the own hand and seen stimulation of the artificial hand must exhibit temporal synchrony. The illusion is not elicited any longer at delays greater than 500 ms [15]. The RHI is explained with the brain resolving the conflict between visual and somatosensory information by integrating multisensory signals leading to the feeling of the rubber hand belonging to the own body [16].

Studies transforming the paradigm into a rubber foot illusion (RFI) show that similar illusions occur in the lower limbs [17]. Some works conclude that multisensory integration processes involved in the elicitation of RFI are similar to the ones found to be responsible for RHI [18], [19]. A direct comparison shows neither qualitative nor quantitative differences in RHI and RFI [20]. However, studies exploring embodiment of artificial lower limbs are scarce in general and examinations considering the complete leg are missing. This paper aims to extend previous knowledge on illusion occurrence in lower limb experimental

Manuscript received January 18, 2018; revised August 24, 2018 and November 24, 2018; accepted January 20, 2019. Date of publication March 19, 2019; date of current version July 13, 2019. This work was supported in part by the German Research Foundation (DFG) through the project "Users' Body Experience and Human–Machine Interfaces in (Assistive) Robotics" under Grant BE 5729/3 and Grant BE 5729/11. P. Overath conducted this work while with the Department of Mechanical Engineering, Technische Universit.t Darmstadt. This paper was recommended by Associate Editor M. Swangnetr Neubert. *(Corresponding author: Philipp Beckerle.)*

D. Penner and J. Vogt are with the Work and Engineering Psychology Research Group, Technische Universität Darmstadt, 64283 Darmstadt, Germany (e-mail: penner@psychologie.tu-darmstadt.de; vogt@psychologie.tu-darmstadt.de).

A. M. H. Abrams is with the Chair of Individual and Technology, RWTH Aachen University, 52062 Aachen, Germany (e-mail: anna.abrams@humtec.rwth-aachen.de).

P. Overath is with Floating Office, 64293 Darmstadt, Germany. He was with the Department of Mechanical Engineering, Technische Universität Darmstadt, Germany (e-mail: overath@stud.tu-darmstadt.de).

P. Beckerle is with the Elastic Lightweight Robotics Group, Robotics Research Institute, Technische Universität Dortmund, 44227 Dortmund, Germany, and also with the Institute for Mechatronic Systems in Mechanical Engineering, Technische Universität Darmstadt, 64287 Darmstadt, Germany (e-mail: philipp.beckerle@tu-dortmund.de).

Color versions of one or more of the figures in this paper are available online at http://ieeexplore.ieee.org.

Digital Object Identifier 10.1109/THMS.2019.2896447

paradigms by examining a robotic leg illusion (RobLI) for the first time. Therefore, a robotic leg was built to experimentally study multisensory integration effects based on previous technical designs proposed in [21] and [22]. According to [23], the feeling of agency in consequence of the actual movement of a video projection of the participants' own hands is an important factor for altered bodily awareness. Moreover, first studies involving robotic limbs derive opportunities to implement interactive human-in-the-loop experiments that enable experimental conditions beyond classical test designs [10]. Experimental versatility and the resemblance of a real hand can be improved [24]–[26]. A study involving a robotic hand even shows stronger illusion effects in active movement conditions [25]. While several studies have shown that robotic systems can elicit robotic hand illusions (RobHI) [25], [27]–[29], a thorough design analysis indicates the complexity of designing proper robotic experiments [26].

The robotic leg presented in this study is specifically designed to investigate the influence of active movements on the illusion. For the first time, an RHI-like paradigm is transferred to the whole leg in general and, especially, during motion. To facilitate these experiments, previous works on the mechatronic design and implementation of a human-in-the-loop system to examine RobLI are extended. Previous solutions investigated in [21] and [22] were limited by system intrinsic delays due to constrained dynamics of the drive trains and due to motion tracking. Section II presents the novel mechatronic design and control, which reduces the delays through remote actuation of the knee joint and inertial sensing of the human motions. A human-in-the-loop study applying the robotic system and a statistically solid dependence analysis give reliable insights in lower limb embodiment, which are presented in Section III and extend knowledge beyond the constrained experiments and merely descriptive analysis in [30]. Section IV gives a detailed discussion on technical as well as psychological aspects. Outcomes are concluded in Section V.

II. Robotic Leg

The mechatronic design and control of the robotic leg is specifically developed to match the requirements of RobLI experiments and based upon prior work in [21] and [22].

A. Mechatronic Design

According to the test design proposed in [21], the robotic leg is implemented as a double-inverted pendulum. As shown in Fig. 1, the lower part mimics the shank while the upper resembles the thigh. For a more natural outer appearance, the leg structure is covered by the hull of a shop-window mannequin and the same trousers as that of the participant according to requirements in [21] and [22]. The joint actuators are controlled to imitate motion of the participant based on motion data acquired by an instrumented knee orthosis that is presented in Fig. 2.

1) Mechanics: While the overall mechanical structure of the leg and the implementation of the ankle joint is identical with those shown in [21] and [22], the knee joint was reworked distinctly to reduce gear play and increase available motor performance. Both supports meeting the temporal and spatial requirements of motion synchronization [26]. Fig. 2(a) shows the knee joint, which is remotely actuated through a Bowden cable. The dc motor that actuates the joint is placed next to the thigh actuator and thereby hidden from the view of the participants as presented in Fig. 2(b). This picture further shows the ankle joint and actuator, which are connected by a timing belt.

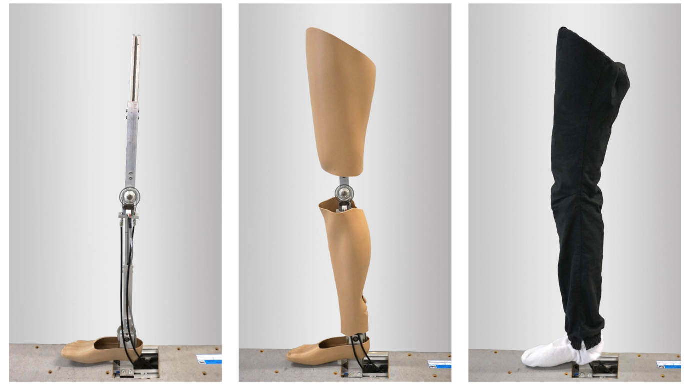

(a) (b) (c)

Fig. 1. (a) Robotic leg with (b) cladding and (c) trousers.

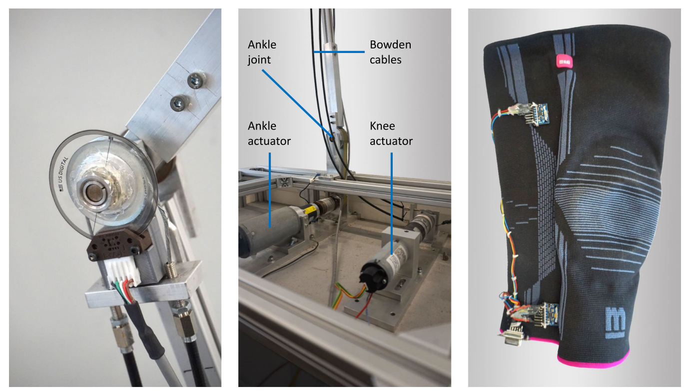

(a) (b) (c)

Fig. 2. Implementation of (a) knee and (b) ankle joints and actuation. (c) Instrumented orthosis.

2) Actuation: The knee joint is driven by a dc motor 1.13.049.401 rated with 20 W supplied by Bühler Motor GmbH, Nürnberg, Germany, and a $i_k = 1{:}60$ planetary gear from Neugart GmbH, Kippenheim, Germany. The drive train is connected to the Bowden cable via a MBK bellows coupling and toothed belt wheels by MÄDLER GmbH, Stuttgart, Germany. The ankle joint is driven by a dc motor 1.13.063.407 rated with 150 W from Bühler Motor GmbH, Nürnberg, Germany. A $1{:}40$ planetary gear from Neugart GmbH, Kippenheim, Germany, and a timing belt with a transmission ratio of $4{:}5$ by Hilger u. Kern Industrietechnik, Mannheim, Germany, provide an overall transmission of $i_a = 1{:}50$.

3) Electronics: The knee and ankle motors are driven by four-quadrant dc servo amplifiers. An LSC 30/2 by Maxon Motor AG, Sachseln, Switzerland, is used for the knee and a VSD-XE 160 by Granite Devices Oy, Tampere, Finland, is applied for the ankle.

The motor motions are measured by incremental encoders. An ME22 from PWB encoders, Eisenach, Germany, with a

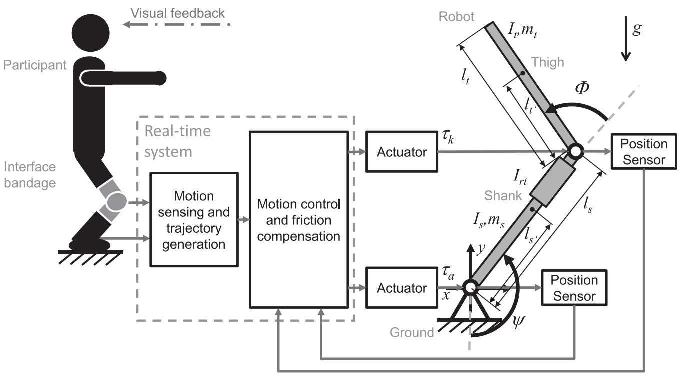

Fig. 3. Sketch of the human–machine system.

resolution of 100 counts per revolution is used to acquire ankle motion, which can be kinematically be transformed into shank motion. For the knee, a 2.648.006 by Bühler Motor GmbH, Nürnberg, Germany, with 100 counts per revolution is applied. Since the Bowden cable might induce an elastic coupling between the motor and the knee joint, an E6 Optical Kit Encoder by US Digital, Vancouver, WA, USA, with 10000 counts per revolution is installed at the robotic knee to measure the thigh position directly. To acquire the motions of the human participant, a Genumedi knee bandage from medi GmbH & Co. KG, Bayreuth, Germany, is equipped with two MPU-6050 inertial measurement units (IMU; each containing an accelerometer and a gyroscope) by InvenSense, San Jose, CA, USA. As shown in Fig. 2(c), one sensor is attached to the thigh and one to the shank. The desired knee and ankle joint angles are computed from the measured thigh and shank orientations.

Sensor acquisition and motion control are implemented on an NI myRIO-1900 real-time control platform from National Instruments Germany GmbH, München, Germany, and operated by a host computer.

B. Modeling and Control

As shown in Fig. 3, the robotic leg is motion controlled and the friction is compensated to imitate the motions of the human subject. To this end, the rotational motions of the participant's shank and thigh are measured via the IMUs. The desired trajectories to be performed by the robotic leg are generated by fusing the accelerometer and gyroscope data via a complementary filter with a cutoff frequency of 0.5 Hz [30]. Through this filter, the desired trajectories are smoothened and more reliable. Subsequently, a dynamics model of the robot is set up and a computed torque controller to track the desired trajectories is devised.

1) Dynamics Model: Neglecting friction effects, the dynamics can be modeled by

$$\tau = M(q)\ddot{q} + C(\dot{q}, q) + G(q) \tag{1}$$

using Lagrange equations of the second kind [31]. The inertial matrix $M(q) = [m_{11}\ m_{12};\ m_{21}\ m_{22}]$ contains the elements given in Table I, whereas the matrices $C(\dot{q}, q)$ and $G(q)$ are

TABLE I
ELEMENTS OF THE INERTIAL MATRIX

Elem.	Content
m_{11}	$I_a + I_t + m_t\ \left(l_s^2 + l_{t'}^2 + 2\, m_t\, l_s\, l_{t'}\ \cos(\phi)\right)$
$m_{12} = m_{21}$	$I_t + m_t\ \left(l_{t'}^2 + l_s\, l_{t'},\ \cos(\phi)\right)$
m_{22}	$I_r t + I_t + m_t\, l_{t'}^2$

TABLE II
PARAMETERS OF MECHANICAL SETUP AND CONTROL

	Parameter	Value	Unit	Description
mechanics	I_a	0.506	kgm^2	reduced ankle inertia
	I_{rt}	0.025	kgm^2	knee actuator inertia
	I_t	0.044	kgm^2	thigh interia
	m_s	0.590	kg	shank mass
	m_t	0.255	kg	thigh mass
	l_s	0.42	m	shank length
	l_t	0.39	m	thigh length
	$l_{s'}$	0.254	m	dist. COM(shank)-ankle
	$l_{t'}$	0.183	m	dist. COM(thigh)-knee
	g	9.81	$\frac{m}{s^2}$	gravity
control	$k_{p,a}$	100	$Nm\ rad^{-1}$	proportional gain, ankle
	$k_{v,a}$	20	$Nm\ s\ rad^{-1}$	derivative gain, ankle
	$k_{p,k}$	256	$Nm\ rad^{-1}$	proportional gain, knee
	$k_{v,k}$	32	$Nm\ s\ rad^{-1}$	derivative gain, knee

specified as

$$C(\dot{q}, q) = \begin{bmatrix} -2\, l_s\, l_{t'}\, m_t\ \sin(\phi)\, \dot{\psi}\, \dot{\phi}\ - l_s\, l_{t'}\, m_t\ \sin(\phi)\, \dot{\phi}^2 \\ m_t\, l_s\, l_{t'}\ \sin(\phi)\, \dot{\psi}^2 \end{bmatrix}$$

$$G(q) = \begin{bmatrix} g\ (l_{t'}\, m_t \sin(\psi + \phi) + (l_{s'}\, m_s + l_s\, m_t)\ \sin(\psi)) \\ g\ (l_{t'}\, m_t\ \sin(\psi + \phi)) \end{bmatrix}.$$

In the dynamic equations, the vectors of angular positions and torques are given by $q = [\psi\ \phi]^T$ and $\tau = [\tau_a\ \tau_k]^T$, respectively. According to [22], I_t denotes the inertia of the thigh with respect to its center of mass and I_{rt} represents the inertia of the rotor in the knee drive. The model parameters given in Table II are determined from the CAD model and weighing particular parts to adjust the model to the real system.

2) Computed Torque Control and Friction Compensation: To control the motions of the robot, computed torque control is combined with a friction compensator. According to [31], the controller implements the analytical inverse dynamics model of the robot as given in (1) including a proportional-derivative (PD) feedback controller

$$\begin{aligned} \tau &= M(q)\ \left[\ddot{q}_d + k_p\, \tilde{q} + k_v\, \dot{\tilde{q}}\right] + C(\dot{q}, q) + G(q) + \tau_{FC} \\ &= \tau_m + C(\dot{q}, q) + G(q) + \tau_{FC}. \end{aligned} \tag{2}$$

Through the friction compensator, the torque τ_{FC} is added. The control parameter matrices are denoted by $k_p = \mathrm{diag}(k_{p,a}\ k_{p,k})$ and $k_v = \mathrm{diag}(k_{v,a}\ k_{v,k})$ and exhibit diagonal structure. The control error between desired and actual motions is given by the vector $\tilde{q} = q_d - q$. Considering an ideal match of the dynamics model and the real robot as well as perfect friction compensation,

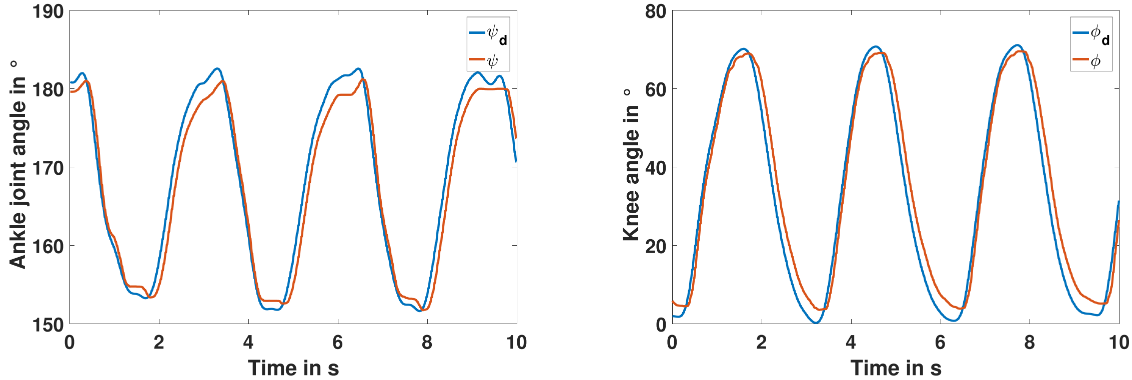

(a) (b)

Fig. 4. Plots of (a) ankle angle ψ (red line) and (b) knee angle ϕ (red line) compared to their desired values ψ_d and ϕ_d (blue lines) during squat experiments to assess the controller.

the linearized closed-loop behavior is given by

$$\ddot{\tilde{q}} + k_v\,\dot{\tilde{q}} + k_p\,\tilde{q} = 0\,. \tag{3}$$

To achieve fast reactions without overshooting in closed-loop behavior, the control parameters are set to $k_p = \omega^2$ and $k_v = 2\,\omega$, where ω is the exponential decay rate of the errors $\tilde{q}$ and $\dot{\tilde{q}}$ [31]. The numeric values leading to the aperiodic boundary case are given in Table II.

For friction compensation, Coulomb and viscous friction are modeled by

$$\tau_F = \tau_C\,\text{sign}(\dot{q}) + a_V\,\dot{q} \tag{4}$$

if $\dot{q} \neq 0$ [32]. The friction-induced torque τ_F includes the Coulomb torque $\tau_C = \text{diag}(0.0203\ \text{N}\cdot\text{m}0.016\text{N}\cdot\text{m})$ for ankle and knee and the product of the viscous friction parameters $a_V = \text{diag}(0.00435\text{N}\cdot\text{m}\cdot rad^{-1}\cdot s^{-1}\ 0.0066\ \text{N}\cdot\text{m}\cdot rad^{-1}\cdot\text{s}^{-1})$ and the vector containing velocities of ankle and knee.

The applied friction compensation algorithm from Rinderknecht and Strah [33] and Beckerle [22] uses a fuzzy-membership function to smoothly superimpose different friction compensation torques depending on joint velocities. The compensation torques are blended considering τ_m and the fuzzy parameters are selected heuristically. Coulomb friction is compensated in case of low velocities and fast switching of the torque direction due to sensor noise is avoided by the fuzzy approach. If velocities are high, Coulomb and viscous frictions are compensated.

3) Controller Evaluation: To assess the control quality of the human–machine system and its suitability for the main experiments regarding embodiment, the response of the system to squat motions performed by one participant were examined. Fig. 4(a) and (b) compares the desired knee and ankle angles in blue to the actual ones given in red. Despite deviations at the peak values, the controller achieves good tracking results. Especially the synchronization of the desired and the actual value is on a very high level, which is crucial to elicit the intended illusion [26]. The plots further outline the squat-to-squat variance, which is caused by alterations in squat conduction by the human.

However, the system intrinsic delay that is caused by the measurements with the instrumented bandage adds upon these values. To assess the delay of the overall system, five squats of a human participant and the robotic leg were filmed with a video camera at a frame rate of 120 Hz. The delay in motion initiation, i.e., starting a squat, is $M_{ai} = 393.18$ ms, $\text{SD}_{ai} = 22.60$ ms for the ankle joint and $M_{ki} = 369.85$ ms, $\text{SD}_{ki} = 18.7$ ms for the knee joint. Regarding motion completion, i.e., arriving at the lowest position, delays of $M_{ac} = 134.95$ ms, $\text{SD}_{ac} = 14.33$ ms and $M_{kc} = 136.61$ ms, $\text{SD}_{kc} = 25.05$ ms are found for the ankle and knee, respectively.

III. Human-in-the-Loop Evaluation

The present study uses a robotic leg to investigate lower limb embodiment for the first time. In contrast to earlier studies considering feet only, the illusion is investigated regarding the whole leg and during motion. According to current knowledge about RHI and RobHI, the study focuses on the multisensory integration and the above-mentioned factors influencing the emergence and strength of the RLI. The following hypotheses were formulated.

Hypothesis 1: If the robotic leg moves synchronously, the proprioceptive drift (PPD) is significantly larger than that with asynchronous movement.

Hypothesis 2: If the robotic leg moves synchronously, the subjectively perceived embodiment is significantly stronger than that with asynchronous movement.

A. Material and Methods

1) Participants: In total, 32 participants were recruited via e-mail and black board notes at Technische Universität Darmstadt. After preanalysis, one participant was dismissed due to outlier scores (4 sigma rule) in the estimation of leg position. The analyses are based on a sample of 31 healthy participants (48.4% male, 51.6% female; average age of $M = 28.26$, standard deviation in age of $\text{SD} = 8.55$). During recruitment, all participants expressed that they were naive to the purpose of the experiment, which was confirmed post hoc considering their questionnaires. All participants provided written, informed consent prior to participation. The study's procedure involving human participants was assessed and positively voted by the ethics commission of Technische Universität Darmstadt. Furthermore, the study is in accordance with the 1964 Helsinki declaration and its later amendments.

2) Experimental Design: A within-subject design was used. Sequence effects were controlled by Latin squares. Two conditions were compared: synchronous control of the robotic leg (synch-near) and asynchronous control of the robotic leg (asynch-near). Additionally, data regarding the influence of distance, i.e., a condition with a larger distance between human and robotic leg (synch-far) motivated in [12], as well as questionnaire items regarding acoustic influences, were collected. In the synchronous conditions, the aspired maximum delay of the robotic leg mimicking the participants' leg movements was 0.1 s [21], [30]. According to Shimada *et al.* [13], the illusion is strongest in case of motion delay of the artificial limb below 0.3 s. Hence, a delay of 0.5 s was chosen for the asynchronous condition. Considering the results of Lloyd [12] and Flögel *et al.* [20], the robotic leg was placed at a distance of 17.5 cm from the real leg in the synch-near and asynch-near conditions and 35 cm for the synch-far condition.

3) Apparatus: The robotic leg has a height of 84 cm, which matches the average height of male population concerning DIN 33402 (male 84.25 cm, female 78 cm) [34]. In addition to the appearance of a human's leg shape, participants were instructed to wear black trousers and sport socks during the experiments same as the robotic leg wore according to [30]. To measure the movements of the participants, the instrumented knee bandage was attached to the participants. Using the computed torque controller, the robotic leg imitated the acquired motion trajectories immediately (synch-near and synch-far) or with the specified delay (asynch-near). A human operator commanded the robotic leg in coordination with the experimenter using a host computer. According to earlier findings [35], [36] concerning the emergence of an illusion by using mirror images, a mirror was installed at the distance of 1.4 m opposite to the setup. The body parts from the hips downward were covered with a cloth. Thus, participants were able to observe their upper body and the robotic leg in the mirror. The whole set up is depicted in Fig. 5.

4) Procedure: After participants had given informed consent, they were instructed verbally and in writing. An exemplary knee bend of 40° was shown to them. Participants were rehearsed to perform squats with a frequency of 0.25 Hz, i.e., to take approximately 4 s for bending their knees, in a brief training session with instructions of the experimenter. The standing position on the base plate was centered on the right foot aligned with the measuring scale. The starting point (0 cm) of the yardstick was the inner side of the robotic foot. Every condition was performed once per participant and included the same steps: twice 15 knee bends followed by a 15-s break of standing in an upright position and again 15 knee bends. Breaks served as regeneration phases for the participants. While moving and pausing, participants directed their gaze toward their image in the mirror. In total, each condition had a duration of 3.5min. Between conditions, participants were instructed to take a break of 5 min to ensure the illusion extinguished completely.

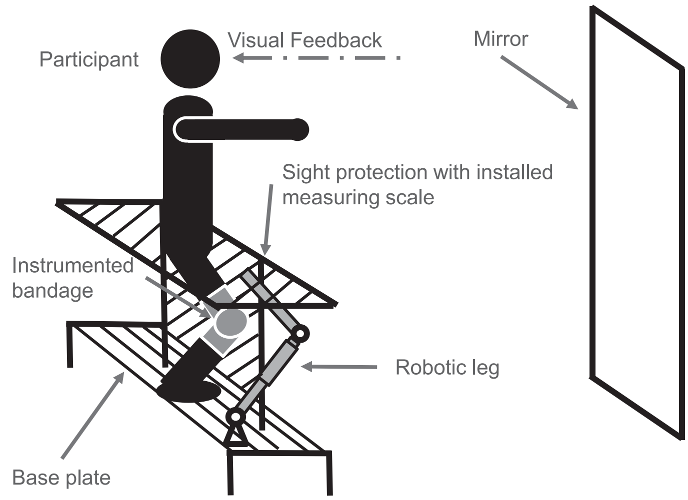

Fig. 5. Sketch of the experimental setup.

5) Measures: After the experiment, every participant was asked to complete the ten-item version of the survey in [37] on a seven-point Likert scale ranging from "1 = Strongly disagree" to "7 = Strongly agree" that an illusion occurred in order to analyze the subjectively experienced illusion. In this questionnaire, participants reported to what extent they feel the artificial hand as part of their own body (ownership), experience its perceived localization (location), and have the feeling to be able to control it (agency). The questionnaire was translated into German and validated for earlier studies [20]. Here, "Roboterbein" (robotic leg) replaced the word "hand." The questionnaire is depicted in Table III.

The intensity of the illusion was assessed objectively using the PPD, i.e., the perceived conversion of the actual limb position and the experienced position typically closer to the artificial limb. Previous RHI studies showed that participants tend to estimate the position of their own hand as 15%–30% closer to the rubber hand than before the experiment [14], [38]. In the present experiment, participants were asked to keep their eyes closed and indicate the center position of their right leg with their index finger. The indicated location was measured on a yardstick before (premeasurement) the experiment and after each condition (postmeasurement). The yardstick was attached to the apparatus at the level of the hip alongside the coronal plane and hidden from participants' view.

6) Analysis: One-way analyses of variances were conducted within subjects searching for significant main effects of the condition (synch-near and asynch-near). Since all statistical assumptions (normal distribution and homogeneity of variances) were given as indicated in Table IV, parametric methods were used to test the hypothesis.

B. Results

According to hypothesis (H1), a synchronous movement (synch-near) would elicit a stronger illusion than an asynchronous movement (asynch-near). A paired sample *t*-test supports this assumption with a significant result $(t(30) =$

TABLE III
ITEMS OF THE QUESTIONNAIRE SCALE MODIFIED FROM [37] IN ENGLISH AND THE TRANSLATED VERSION IN GERMAN, WHICH WERE USED IN THE STUDY

	Original statement During the block...	Translated item Während der Durchführung...
1.	...It seemed like I was looking directly at my own leg, rather than at a robotic leg.	...Schien es, als schaute ich eher auf mein eigenes statt auf ein Roboterbein.
2.	...It seemed like the robotic leg began to resemble my real leg.	...Schien es, als würde das Roboterbein beginnen, meinem echten zu ähneln.
3.	...It seemed like the robotic leg belonged to me.	...Schien es, als gehöre das Roboterbein zu mir.
4.	...It seemed like the robotic leg was my leg.	...Schien es, als sei das Roboterbein mein eigenes.
5.	...It seemed like the robotic leg was part of my body.	...Schien es, als sei das Roboterbein Teil meines Körpers.
6.	...It seemed like my leg was in the location where the robotic leg was.	...Schien es, als befand sich mein eigenes Bein dort, wo das Roboterbein war.
7.	...It seemed like the robotic leg was in the location where my leg was.	...Schien es, als befand sich das Roboterbein dort, wo mein echtes Bein war.
8.	...It seemed like a touch on the robotic leg I would perceive as a touch on my own leg.	...Schien es, als könnte ich Berührungen am Roboterbein als Berührungen an meinem echten Bein wahrnehmen.
9.	...It seemed like I could have moved the robotic leg if I had wanted.	...Schien es, als könne ich das Roboterbein bewegen, wenn ich wollte.
10.	...It seemed like I was in control of the robotic leg.	...Schien es, als habe ich die Kontrolle über das Roboterbein.

TABLE IV
RESULTS OF THE NORMAL DISTRIBUTION EXAMINATION FOR ALL DEPENDENT VARIABLES IN THE NEAR CONDITIONS

		synch-near	asynch-near
Survey	Statistic (p)	0.97(0.500)	0.96(0.348)
Pre-measurement (PPD)	Statistic (p)	0.97(0.638)	0.95(0.132)
Post-measurement (PPD)	Statistic (p)	0.96(0.211)	0.97(0.396)
Difference (PPD)	Statistic (p)	0.97(0.553)	0.96(0.213)

5.447, $p < .001$). As depicted in the top diagram of Fig. 6, a shift of localizing the own leg (PPD) toward the robotic leg can be seen from premeasurement ($M_{\text{synch-near}} = 24.31$, $\text{SD}_{\text{synch-near}} = 3.23$) to postmeasurement ($M_{\text{synch-near}} = 21.86$, $\text{SD}_{\text{synch-near}} = 4.36$). Comparisons between premeasurement ($M_{\text{asynch-near}} = 23.28$, $\text{SD}_{\text{asynch-near}} = 3.92$) and postmeasurement ($M_{\text{asynch-near}} = 24.50$, $\text{SD}_{\text{asynch-near}} = 3.63$) in the asynch-near condition indicate a drift away from the robotic leg. The total difference in centimeters was calculated by subtracting postmeasurement results from premeasurement results and is presented in the bottom diagram in Fig. 6.

H2 postulated the subjectively perceived embodiment to be stronger in a synchronous condition (synch-near). The significance of the difference between the two synchronous conditions

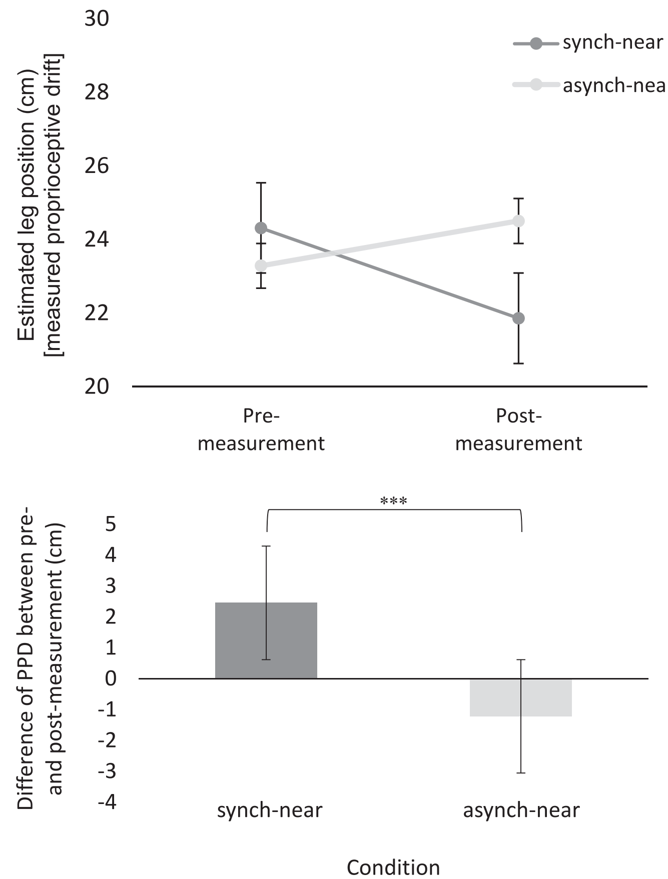

Fig. 6. Comparison between the premeasurement and postmeasurement in the PPD toward the robotic leg: Mean of the estimated position of the real leg before (premeasurement) and after (postmeasurement) the induction of the illusion (top). Mean difference between the premeasurement and postmeasurement according to the conditions synch-near and asynch-near (bottom). Error bars represent standard errors.

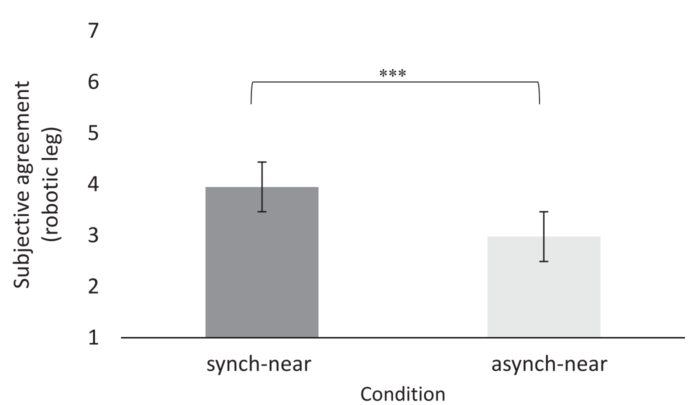

Fig. 7. Comparison of means (bars) and standard deviations (whiskers) regarding the subjectively experienced integration of the robotic leg into the own body schema between the conditions synch-near and asynch-near.

($t(30) = 5.523$, $p < .001$) based on the questionnaire items is shown in Fig. 7, which supports this hypothesis.

C. Potential Influencing Factors

As a preliminary step toward examining further factors that could potentially influence embodiment, the factors distance, which is related to the peripersonal space, and acoustics were taken into account.

Considering Rizzolatti *et al.* [39], the brain parts involved in constructing the spatial body representation will most likely respond to the RobLI when the leg is within the peripersonal space and in an anatomically plausible position. Following Lloyd [12], the strongest illusion can be expected distances of 15–30 cm and the effect should decay beyond. To check if there might be effects due to the distance between human and robot, a comparison of the synch-near and synch-far was performed. A paired sample *t*-test shows no significant difference neither for PPD ($t(30) = 0.898$, $p = 0.376$; premeasurement ($M_{\text{synch-far}} = 40.28$, $\text{SD}_{\text{synch-far}} = 3.45$; $M_{\text{synch-near}} = 24.31$, $\text{SD}_{\text{synch-near}} = 3.23$); postmeasurement ($M_{\text{synch-far}} = 38.55$, $\text{SD}_{\text{synch-far}} = 5.24$; $M_{\text{synch-near}} = 21.86$, $\text{SD}_{\text{synch-near}} = 4.36$)) nor for subjectively perceived embodiment ($t(30) = 0.018$, $p = 0.986$; ($M_{\text{synch-near}} = 3.95$, $\text{SD}_{\text{synch-near}} = 1.20$; $M_{\text{synch-far}} = 3.95$, $\text{SD}_{\text{synch-far}} = 1.26$)) between the conditions synch-near and synch-far.

In the closing demographic questionnaire, 29 participants reported to have consciously perceived the sound of the robotic hardware throughout the experiment. Half of the participants (15) classified the noise as disturbing.

IV. Discussion

The results of this paper are discussed considering the mechatronic implementation of the robotic leg and the results of the human-in-the-loop evaluation.

A. Robotic Leg

Compared to the previous studies such as [22] and [30], the mechatronic implementation of the robotic leg improved in various directions. A key improvement is the remote actuation of the knee joint, which allows us to use a motor with higher power. Due to using a collocated sensor, i.e., the knee encoder, control quality increases distinctly despite the elasticity of the applied Bowden cable. Regarding the ankle, the implementation is not changed compared to [21] and [22].

The acquired human motion through the instrumented knee bandage instead of an RGB-D sensor [21] decreases the computational effort to interpret measured data. Hence, a control platform with less computational power is sufficient to command the actuators and, more importantly, the system-intrinsic delay could be reduced distinctly compared to [22]. While the delays for motion initiation could be critical concerning the elicitation of the illusion, the delays for motion completion appear acceptable. Yet, the results of the human-in-the-loop evaluation show that the illusion was elicited. Hence, the improvements of mechatronic implementation facilitate appropriate human-in-the-loop experiments according to requirements determined in [21], [22], and [26]. It has to be noted that creating the reference trajectory from the measured healthy leg motion differs from the situation encountered in prosthetics. Hence, results with an existing human–machine interface are not directly transferable to prosthetic application, but indicate that the robotic system is a feasible research vessel to investigate modulating factors of embodiment and can be equipped with future interfaces, e.g., electromyographic control [40].

B. Human-in-the-Loop Evaluation

This study transferred RHI to a complete robotic leg for the first time. Beyond the novelty of using the robotic leg to investigate artificial limb illusions, motion was rarely included in these paradigms before. The current technical setup derives opportunities for investigation of embodiment through active movement.

The results show that synchronous movement (synch-near) elicited an illusion. Both, subjective and objective measures, give significant evidence that an illusion emerged. The effect was significantly weaker in the condition with asynchronous movement of the robot (asynch-near). Results indicate synchrony to be a relevant factor for lower as well as for upper extremities in elicitation of an illusion and subsequently an embodiment of foreign objects [14], [18], [20], and [37]. Asynchronous movement led to a negative result ($M = -1.22$) meaning that the participants experienced the robotic leg to be further away.

Furthermore, auditory perception of sounds of the robotic limb might have an effect. Outlooking to upcoming experiments, designs should also take into account that how auditory stimuli influence bodily illusions and body schema integration. Audition might be especially important for our legs, as we perceive our steps as a proof of constant movement and belonging. According to [41] and [42], the representation of the peripersonal space can be influenced by auditory feedback. If an auditory stimulus is within a certain distance (peripersonal space), it can lead to feelings of belonging. Most participants experience that the rubber hand has become part of their body when the artificial object is in an anatomically plausible position to the real hand and within a distance of maximally 0.3 m [11]–[14]. This sense is only strengthened through active movement and control [43]. Additionally, watching the robotic leg move in accordance to one's own movement probably strengthened the effect. The consciousness to be able to move the leg might lead to an extension of the peripersonal space through multisensory integration [44]. Yet, these factors, auditory perception, and peripersonal space, are still to be explored. Moreover, to examine if the fixed height of robotic leg influences the results, the adjustable mechanism of the leg segments could be used. In this study, the specific height of robotic leg represented the average height of male population 84 cm. Individuals with body heights below and above average might experience a less intensive illusion due to the deviating appearance of the robot.

Concerning multisensory integration, further studies should concentrate on the relevance of visual-tactile and audio-tactile factors. This is supported by studies indicating that spatial perception is weaker when auditory and tactile stimuli interact [45], [46] than when visual and tactile stimuli interact [47], [48]. RHI and RLI could be fruitful paradigms to study the relationship of those multisensory components.

Considering the insights of the experiments, further studies should be full factorial to understand interaction between visuomotor synchrony and distance and might examine other scenarios. This could be achieved by modifying the robotic leg to perform knee lifts instead of knee bends. Hence, the artificial leg would be present in participant's frame without continuously staring and focusing on it. Additionally in such an experimental setup, the mirror would be dispensable.

V. Conclusion

This paper presents a robotic leg device that facilitates human-in-the-loop exploration of body schema integration with regard to the lower limbs. For the first time, the RHI is transferred to the whole leg in general and during motion. Through improvements of the mechatronic system, system-intrinsic delay is reduced compared to the previous system. Consequently, most participants integrated the robotic leg into their body schema in the evaluation study, which underlines the importance of motion synchronization. Moreover, results imply that influences from acoustic stimulation should be investigated. In addition, the robotic device can be used to further explore the peripersonal space. Since human-in-the-loop experiments enable precise alterations of multisensory interaction between proprioceptive, visual, and tactile stimuli during motion, future studies are expected to shed light on other challenging aspects of human body experience and support design of human-centered assistive robotic devices.

Acknowledgment

The authors would like to thank Bühler Motor GmbH and medi GmbH & Co. KG for hardware donations.

References

[1] T. M. Cutson and D. R. Bongiorni, "Rehabilitation of the older lower limb amputee: A brief review," *J. Amer. Geriatrics Soc.*, vol. 44, no. 11, pp. 1388–1393, 1996.

[2] B. Rybarczyk, J. Nicholas, and D. Nyenhuis, "Coping with a leg amputation: Integrating research and clinical practice," *Rehabil. Psychol.*, vol. 42, no. 3, pp. 241–256, 1997.

[3] P. Beckerle, O. Christ, T. Schürmann, J. Vogt, O. von Stryk, and S. Rinderknecht, "A human–machine-centered design method for (powered) lower limb prosthetics," *Robot. Auton. Syst.*, vol. 95, pp. 1–12, 2017.

[4] M. Windrich, M. Grimmer, O. Christ, S. Rinderknecht, and P. Beckerle, "Active lower limb prosthetics: A systematic review of design issues and solutions," *BioMed. Eng. OnLine*, vol. 15, no. 3, pp. 5–19, 2016.

[5] H. Senra, R. A. Oliveira, I. Leal, and C. Vieira, "Beyond the body image: A qualitative study on how adults experience lower limb amputation," *Clin. Rehabil.*, vol. 26, no. 2, pp. 180–191, 2012.

[6] A. Mayer, K. Kudar, K. Bretz, and J. Tihanyi, "Body schema and body awareness of amputees," *Prosthetics Orthotics Int.*, vol. 32, no. 3, pp. 363–382, 2008.

[7] P. Haggard and D. M. Wolpert, "Disorders of body scheme," in *Proc. Higher-Order Motor Disorders: From Neuroanatomy and Neurobiology to Clinical Neurology*, H. J. Freund, M. Jeannerod, M. Hallett, and R. Leiguarda, Eds. Oxford, U.K.: Oxford Univ. Press, 2005.

[8] M. R. Longo, F. Schüür, M. P. Kammers, M. Tsakiris, and P. Haggard, "Self awareness and the body image," *Acta Psychologica*, vol. 132, no. 2, pp. 166–172, 2009.

[9] M. Botvinick and J. Cohen, "Rubber hands 'feel' touch that eyes see," *Nature*, vol. 391, no. 6669, pp. 756–756, 1998.

[10] P. Beckerle, C. Castellini, and B. Lenggenhager, "Robotic interfaces for cognitive psychology and embodiment research: A research roadmap (in press)," *WIREs Cogn. Sci.*, vol. 10, no. 2, 2019, Art. no. e1486.

[11] H. Holle, N. McLatchie, S. Maurer, and J. Ward, "Proprioceptive drift without illusions of ownership for rotated hands in the "rubber hand illusion" paradigm," *Cogn. Neurosci.*, vol. 2, no. 3/4, pp. 171–178, 2011.

[12] D. M. Lloyd, "Spatial limits on referred touch to an alien limb may reflect boundaries of visuo-tactile peripersonal space surrounding the hand," *Brain Cogn.*, vol. 64, no. 1, pp. 104–109, 2007.

[13] S. Shimada, K. Fukuda, and K. Hiraki, "Rubber hand illusion under delayed visual feedback," *PloS One*, vol. 4, no. 7, 2009, Art. no. e6185.

[14] M. Tsakiris and P. Haggard, "The rubber hand illusion revisited: Visuotactile integration and self-attribution," *J. Exp. Psychol., Hum. Perception Perform.*, vol. 31, no. 1, pp. 80–91, 2005.

[15] M. Rohde, M. Di Luca, and M. O. Ernst, "The rubber hand illusion: feeling of ownership and proprioceptive drift do not go hand in hand," *PloS One*, vol. 6, no. 6, 2011, Art. no. e21659.

[16] A. Kalckert and H. H. Ehrsson, "The moving rubber hand illusion revisited: Comparing movements and visuotactile stimulation to induce illusory ownership," *Consciousness Cogn.*, vol. 26, pp. 117–132, 2014.

[17] O. Christ, A. Elger, K. Schneider, P. Beckerle, J. Vogt, and S. Rinderknecht, "Identification of haptic paths with different resolution and their effect on body scheme illusion in lower limbs," in *Proc. Technically Assisted Rehabil.*, 2013.

[18] B. Lenggenhager, L. Hilti, and P. Brugger, "Disturbed body integrity and the "rubber foot illusion"," *Neuropsychology*, vol. 29, no. 2, pp. 205–211, 2015.

[19] S. Crea, M. D'Alonzo, N. Vitiello, and C. Cipriani, "The rubber foot illusion," *J. NeuroEng. Rehabil.*, vol. 12, 2015, Art. no. 77.

[20] M. Flögel, K. T. Kalveram, O. Christ, and J. Vogt, "Application of the rubber hand illusion paradigm: Comparison between upper and lower limbs," *Psychol. Res.*, vol. 80, no. 2, pp. 298–306, 2016.

[21] P. Beckerle *et al.*, "Design and control of a robot for the assessment of psychological factors in prosthetic development," in *Proc. IEEE Int. Conf. Syst., Man, Cybern.*, 2012, pp. 1485–1490.

[22] P. Beckerle, F. Schültje, J. Wojtusch, and O. Christ, "Implementation, control and user-feedback of the int^{2}bot for the investigation of lower limb body schema integration," in *Proc. IEEE Int. Symp. Robot Hum. Interact. Commun.*, 2014, pp. 704–709.

[23] M. Tsakiris, G. Prabhu, and P. Haggard, "Having a body versus moving your body: How agency structures body-ownership," *Consciousness Cogn.*, vol. 15, no. 2, pp. 423–432, 2006.

[24] A. De Beir, E. Caspar, F. Yernaux, P. M. D. S. da Gama, B. Vanderborght, and A. Cleermans, "Developing new frontiers in the rubber hand illusion: Design of an open source robotic hand to better understand prosthetics," in *Proc. IEEE Int. Symp. Robot Hum. Interact. Commun.*, 2014, pp. 905–910.

[25] E. A. Caspar, A. de Beir, P. A. Magalhães Da Saldanha da Gama, F. Yernaux, A. Cleeremans, and B. Vanderborght, "New frontiers in the rubber hand experiment: When a robotic hand becomes one's own," *Behav. Res. Methods*, vol. 47, no. 3, pp. 744–755, 2015.

[26] P. Beckerle, A. De Beir, T. Schürmann, and E. A. Caspar, "Human body schema exploration: Analyzing design requirements of robotic hand and leg illusions," in *Proc. IEEE Int. Symp. Robot Hum. Interact. Commun.*, 2016, pp. 763–768.

[27] J. Arata, M. Hattori, S. Ichikawa, and M. Sakaguchi, "Robotically enhanced rubber hand illusion," vol. 7, no. 4, pp. 526–532, Oct.–Dec. 2014.

[28] R. Romano, E. Caffa, A. Hernandez-Arieta, P. Brugger, and A. Maravita, "The robot hand illusion: Inducing proprioceptive drift through visuomotor congruency," *Neuropsychologia*, vol. 70, pp. 414–420, 2015.

[29] M. Hara, H. Nabae, A. Yamamoto, and T. Higuchi, "A novel rubber hand illusion paradigm allowing active self-touch with variable force feedback controlled by a haptic device," *IEEE Trans. Hum.-Mach. Syst.*, vol. 46, no. 1, pp. 78–87, Feb. 2016.

[30] T. Schürmann, P. Overath, O. Christ, J. Vogt, and P. Beckerle, "Exploration of lower limb body schema integration with respect to body-proximal robotics," in *Proc. IEEE Int. Forum Res. Technol. Soc. Ind.*, 2015, pp. 61–65.

[31] R. Kelly, V. Santibáñez Davila, and J. A. Loría Perez, *Control of Robot Manipulators in Joint Space*. New York, NY, USA: Springer, 2005.

[32] B. Bona and M. Indri, "Friction compensation in robotics: An overview," in *Proc. IEEE Conf. Decis. Control, Eur. Control Conf*, 2005, pp. 4360–4367.

[33] S. Rinderknecht and B. Strah, "Simple and effective friction compensation on wheeled inverted pendulum systems," in *Proc. Euro-Mediterranean Conf. Struct. Dyn. Vibroacoust.*, 2013.

[34] H. W. Jürgens, "Erhebung anthropometrischer Maße zur Aktualisierung der DIN 33 402. Teil 2," in *Proc. Schriftenreihe der Bundesanstalt für Arbeitsschutz und Arbeitsmedizin: Forschungsbericht, Fb 1023*, Wirtschaftsverlag NW Verlag für neue Wissenschaft GmbH, 2004.

[35] J. P. Hunter, J. Katz, and K. D. Davis, "The effect of tactile and visual sensory inputs on phantom limb awareness," *Brain*, vol. 126, no. 3, pp. 579–589, 2003.

[36] V. S. Ramachandran and W. Hirstein, “The perception of phantom limbs. The D. O. Hebb lecture,” *Brain*, vol. 121, no. 9, pp. 1603–1630, 1998.

[37] M. R. Longo, F. Schüür, M. P. Kammers, M. Tsakiris, and P. Haggard, “What is embodiment? A psychometric approach,” *Cognition*, vol. 107, no. 3, pp. 978–998, 2008.

[38] T. R. Makin, N. P. Holmes, and H. H. Ehrsson, “On the other hand: dummy hands and peripersonal space,” *Behav. Brain Res.*, vol. 191, no. 1, pp. 1–10, 2008.

[39] G. Rizzolatti, C. Scandolara, M. Matelli, and M. Gentilucci, “Afferent properties of periarcuate neurons in macaque monkeys. II. visual responses,” *Behav. Brain Res.*, vol. 2, no. 2, pp. 147–163, 1981.

[40] C. Castellini *et al.*, “Proceedings of the first workshop on peripheral machine interfaces: Going beyond traditional surface electromyography,” *Frontiers Neurorobot.*, vol. 5, no. 22, pp. 1–17, 2014.

[41] J. E. Aspell, B. Lenggenhager, and O. Blanke, “Keeping in touch with one’s self: Multisensory mechanisms of self-consciousness,” *PloS One*, vol. 4, no. 8, 2009, Art. no. e6488.

[42] E. Macaluso, N. George, R. Dolan, C. Spence, and J. Driver, “Spatial and temporal factors during processing of audiovisual speech: A pet study,” *NeuroImage*, vol. 21, no. 2, pp. 725–732, 2004.

[43] E. Canzoneri, S. Ubaldi, V. Rastelli, A. Finisguerra, M. Bassolino, and A. Serino, “Tool-use reshapes the boundaries of body and peripersonal space representations,” *Exp. Brain Res.*, vol. 228, no. 1, pp. 25–42, 2013.

[44] A. Iriki, M. Tanaka, and Y. Iwamura, “Coding of modified body schema during tool use by macaque postcentral neurones,” *Neuroreport*, vol. 7, no. 14, pp. 2325–2330, 1996.

[45] M. Bassolino, A. Serino, S. Ubaldi, and E. Ladavas, “Everyday use of the computer mouse extends peripersonal space representation,” *Neuropsychologia*, vol. 48, no. 3, pp. 803–811, 2010.

[46] A. Serino, M. Bassolino, A. Farne, and E. Ladavas, “Extended multisensory space in blind cane users,” *Psychol. Sci.*, vol. 18, no. 7, pp. 642–648, 2007.

[47] C. Spence, F. Pavani, and J. Driver, “Crossmodal links between vision and touch in covert endogenous spatial attention,” *J. Exp. Psychol.: Hum. Perception Perform.*, vol. 26, no. 4, pp. 1298–1319, 2000.

[48] J. M. Yau, J. B. Olenczak, J. F. Dammann, and S. J. Bensmaia, “Temporal frequency channels are linked across audition and touch,” *Current Biol.*, vol. 19, no. 7, pp. 561–566, 2009.

Dimitri Penner received the Master of Science degree in psychology from the Technische Universität (TU) Darmstadt, Darmstadt, Germany, in 2017.

Since 2017, he has been a Research Associate with the Work and Engineering Psychology Research Group, TU Darmstadt. His main research interests are human–machine interaction, human–computer interaction, and their usability.

Anna M. H. Abrams received the Master’s degree in engineering psychology from the Technische Universität Darmstadt, Darmstadt, Germany, in 2016.

She is currently conducting her doctoral research at the Chair of Individual and Technology, RWTH Aachen University, Aachen, Germany. Her research interests include social and cognitive factors in human–robot interaction.

Philipp Overath received the Master’s degree in mechatronics from the Technische Universität Darmstadt, Darmstadt, Germany, in 2018.

He is a cofounder of the start-up company Floating Office, developing a new type of height-adjustable desk.

Joachim Vogt received the Dr. Phil. degree in psychology from the Technische Universität Dortmund, Dortmund, Germany, in 1998.

Since 2009, he has been a Full Professor and Head of the Work and Engineering Psychology Research Group, Technische Universität Darmstadt, Darmstadt, Germany. His main research interests are ergonomics, human–machine systems, psychophysiology, safety, and (cyber)security.

Philipp Beckerle (M’12) received the Dr.-Ing. degree in mechatronics from the Technische Universität Darmstadt, Darmstadt, Germany, in 2014.

He is currently an Assistant Professor with the Elastic Lightweight Robotics Group, Technische Universität Dortmund, Dortmund, Germany, and an Adjunct Researcher with the Technische Universität Darmstadt. He was a visiting researcher with the Robotics and Multibody Mechanics Research Group, Vrije Universiteit Brussel, Interactive Robotics Lab and Human-Oriented Robotics and Control Lab, Arizona State University, and Human Centered Robotics Group, University of Siena. He takes over review and editorial responsibilities for various international journals and conferences. His main research topics are human–machine centered design, elastic actuation, wearable robotics, and human–robot interaction.

Dr. Beckerle’s dissertation was awarded the Manfred-Hirschvogel Award 2015 and the MINT Excellence Ph.D. thesis award 2015. He was the recipient of the Eugen-Hartmann Award 2017 and the Athene Young Investigator grant in 2017.